Adaptive correction for airborne electromagnetic measurements

Andrey Volkovitsky
Institute of Control Sciences
65 Profsoyuznaya street, Moscow
avolkovitsky@yandex.ru

Evgeny Karshakov
Institute of Control Sciences
65 Profsoyuznaya street, Moscow
karshakov@ipu.ru

SUMMARY

We present results of development and practical implementation of the adaptive correction method and algorithm. They ensure high accuracy and stability of the airborne low-frequency inductive electromagnetic measurements. We describe the theoretical foundations of the method and the basic schemes of the algorithm, and consistently consider the stages of computational transformations. We provide several examples of experimentally obtained data proving the effectiveness of the method. The main result achieved is the possibility of functioning of the airborne electromagnetic system without calibration during the entire flight.

Key words: measurements transformations; frequency domain; adaptive correction.

INTRODUCTION

Modern trends of development of the AEM technologies set ever higher demands on the detail and accuracy of measurements (Legault, 2015). It is directly related to the problem of suppression of distortions of various kinds during the measurements processing. The influence of the measurement distortions is especially strong for inductive low-frequency AEM systems. The impact is harmful because the induced field at the location of the receiver overwhelms the response from the conductive layers of the medium. And the receiver registers both these fields simultaneously. Under these conditions, the inherent instability of the measurement conversion parameters has a decisive influence.

The interpretation reliability, as well as the productivity of the survey, are significantly limited since the required accuracy is achievable only in a time interval between calibration procedures. Calibration is usually done at a high enough altitude where the secondary field can be neglected. Reducing the number of such procedures during the flight is our main goal.

It is assumed that modern AEM systems must solve very complex problems, such as estimation of induced polarization and superparamagnetic parameters (Macnae, 2016). And for this we need to carefully eliminate all possible noises. The survey of existing approaches can be found in Wu et al. (2019). From their work, it can be concluded that it is necessary to ensure the sensitivity of the receiver at a level of the order of 10^{-6} with respect to the primary field. The authors considered various noises, including motion-induced noise, nearby or moderately distant sferics noise, power-line noise, background electromagnetic noise etc. They proved that sensitivity at this level is achievable.

At the same time it is absolutely impossible to ensure the stability of measurements with such an accuracy at the hardware level even using the most modern electronic elements. Here we propose a method and an algorithm for stabilizing the measurement accuracy.

THE ADAPTIVE CORRECTION IDEA

We can ensure the accuracy and stability of measurement transformations by digital filtering, applied during registration,which may significantly reduce noises (Hemming, 2013). In frequency domain having a continuous sounding field the measurement results are usually presented in the form of coherent accumulation:

$$U(t_0, j\omega_k) = \frac{1}{2N+1} \sum_{n=-N}^{N} f_n \cdot e^{j\omega_k t_n} u(t_0, t_n). \qquad (1)$$

Here $U(t_0, j\omega_k)$ are the complex amplitudes for all sounding frequencies ω_k, $t_n = t_0 + n\Delta\tau$, $\Delta\tau$ is the time step of analog to digital conversion, $2N+1$ is the number of samples in the averaging interval.

Coherent accumulation, or synchronous detection, has an important feature of frequency selectivity as applied to AEM signals processing. The detection results turn out to be insensitive not only to signals that are significantly far from the detection frequency in frequency domain, but also to signals with frequencies that are separated from it by a strictly defined frequency interval, which depends entirely on the shape of the weight function f_n (Figure 1). In the figure δ is the frequency interval strickely defined by the form of f_n. Signals at frequencies $\omega_k \pm \delta$ close to the main one ω_k turn out to be invisible after applying (1).

At these invisible frequencies a set of reference signals can be added to the input of the system, since it will not affect the results of detecting the main frequencies.

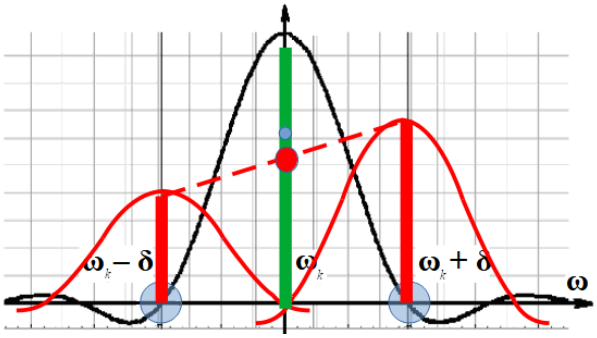

Figure 1. Selectivity of coherent accumulation main signal (green), reference signals (red), frequency response of the filter f_n

Then, by accumulating each reference signal on the system output and assuming the frequency band of the resulting triplet is narrow, we are able to get the value of the frequency response of the conversion at the main frequency. Figure 1 shows the form of the frequency response of coherent accumulation, the spectral lines of the reference process, the scheme of calculating the conversion coefficient for main detection frequency.

ALGORITHM OF ADAPTIVE CORRECTION FOR FREQUENCY DOMAIN AEM

Let us consider the operation of the adaptive correction method and algorithm for a harmonic field of a frequency ω_k. Having equation (1) we can also consider the result in the following form:

$$U(t, j\omega_k) = W(t, j\omega_k) \cdot X(t, j\omega_k), \qquad (2)$$

where $W(t, j\omega_k)$ is the measurement transformation applied to the input signal $X(t, j\omega_k)$.

Applying (1) at the frequencies $\omega_k \pm \delta$ we will not see the input signal $X(t, j\omega_k)$, while ω_k is shifted by δ. Nevertheless, we will be able to see the left (L) and the right (R) reference signals:

$$\begin{aligned} U_L(t, j\omega_k) &= W(t, j(\omega_k - \delta)) \cdot X_L(j\omega_k), \\ U_R(t, j\omega_k) &= W(t, j(\omega_k + \delta)) \cdot X_R(j\omega_k). \end{aligned} \qquad (3)$$

We have to note that $X_L(j\omega_k)$, $X_R(j\omega_k)$ are actually related to the frequencies $\omega_k - \delta$, and $\omega_k + \delta$ respectively. But while these signals are associated with the main frequency ω_k, we will not write δ in the argument. Also these signals supposed to be stationary, so they do not depend on time. So, only W contains t as an argument in the last two equations.

It is important that the proposed method allows us to obtain for the same coherent accumulation interval both the value of the complex amplitude of the signal and the parameters of the measurement transformation W for the known stationary signal. So, using the reference signals X_L and X_R the approximate value of W can be calculated as

$$\widetilde{W}(t, j\omega_k) = \frac{1}{2}\left(\frac{U_L(t, j\omega_k)}{X_L(j\omega_k)} + \frac{U_R(t, j\omega_k)}{X_R(j\omega_k)}\right). \qquad (4)$$

This makes it possible to track the variability of measurement transform coefficient and correct the main signal as follows:

$$\widetilde{X}(t, j\omega_k) = \frac{U(t, j\omega_k)}{\widetilde{W}(t, j\omega_k)}. \qquad (5)$$

So, for the same accumulation interval, both the approximate value of the conversion coefficient $\widetilde{W}(t, j\omega_k)$ for the frequency ω_k and the corrected value of the complex amplitude of the main signal $\widetilde{X}(t, j\omega_k)$ for this frequency are obtained.

ALGORITHM OF ADAPTIVE CORRECTION FOR TIME DOMAIN AEM

For AEM methods the sounding field is usually periodic and its frequency spectrum is discrete. When the sounding signals sequentially switching polarity pulses, spectrum has only odd harmonics (Figure 2).

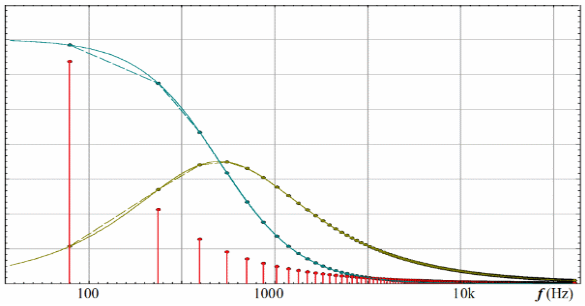

Figure 2. Structure of the sounding spectrum

For the spectrum structure, each of the lines can have its own pair of reference frequencies. It becomes a set of triplets, and for each one correction can be performed according to the above scheme (4)–(5).

In case of time domain measurements we are able to apply Fourier transform to the measured data. After that we can deal with them as with frequency domain data, including adaptive correction. While both digital filtering and Fourier transform are linear operations, we can switch the summation order to separate main and reference signals. Obviously, having in (1)

$$u(t_0, t_n) = \frac{1}{K}\sum_{k=1}^{K} U(t_0, j\omega_k) \cdot e^{j\omega_k t_n}, \qquad (6)$$

we can apply all the described techniques to each frequency separately. But to add the reference signals, we recommend using the following method for generating them

$$X_{LR}(t_n) = \cos(\delta t_n) \sum_{k=1}^{K} A_k \cdot \cos(k\omega_0 t_n). \qquad (7)$$

In this case it is easy to show that $X_{LR}(t_n) = (X_L(t_n) + X_R(t_n))/2$. In frequency domain for each frequency $k\omega_0$, $k = 1,\ldots,K$, $X_L(jk\omega_0) = X_R(jk\omega_0) = X_{LR}(jk\omega_0)$. The value of ω_0 is the base frequency of the system – the lowest frequency of the primary field spectrum.

We can note, that formula (7) approximates an impulse function. But it works for any other. The key idea here is to modulate it with the frequency δ to make it invisible for filtering with f_n.

To extract the reference signal, we modulate the measured signal $u(t)$ with the frequency δ of the interval between the main and the reference harmonics.

$$u_M(t_0) = \frac{1}{2N+1}\sum_{n=-N}^{N} f_n \cdot \cos(\delta t_n) u(t_0, t_n). \qquad (8)$$

Due to the mentioned properties of the filter f_n the detection result will not contain the signal at any of main frequencies $k\omega_0$, $k = 1,\ldots,K$.

Indeed, using (7) as a signal, we'll get $\cos^2(\delta t_n)$ in (8), so the result will be similar to $X_{LR}(t_n)$ with a scale factor. A stationary non modulated signal containing only $k\omega_0$ harmonics will give zero as the result, while any of those harmonics after multiplying by $\cos(\delta t_n)$ gives a sum of harmonics of $k\omega_0 \pm \delta$ frequencies.

Using Fourier transform, frequency domain shape of the output signals can be obtained for both the main signal and the reference signals. Due to selectivity of the coherent accumulation in spectral form the detection result gives the frequency response of measuring conversion up to a known factor X_{LR}:

$$U_M(t,j\omega_k) = \frac{W(j(\omega_k-\delta))+W(j(\omega_k+\delta))}{2} X_{LR}(j\omega_k),$$
$$\tilde{W}(j\omega_k) = \frac{U_M(t,j\omega_k)}{X_{LR}(j\omega_k)}. \quad (9)$$

Now, for the main signal at all frequencies of the spectrum, according to (5), a correction can be performed, after which, using the inverse Fourier transform, the original time domain form for the main process is restored:

$$\tilde{X}(t,j\omega_k) = \frac{U(t,j\omega_k)}{\tilde{W}(t,j\omega_k)},$$
$$\tilde{x}(t,t_n) = \frac{1}{K}\sum_{k=1}^{K} \tilde{X}(t,j\omega_k)\cdot e^{j\omega_k t_n}. \quad (10)$$

PRACTICAL IMPLEMENTATION

Let's consider the results of the adaptive correction method on the example of data obtained for the EQUATOR AEM system (Moilanen *et al.*, 2013).

To implement the method and the algorithm, an additional transmitter dipole as a source of the reference magnetic field is built into the receiver. The current in this dipole is induced using a precise digital-to-analog conversion. Time-domain form of the reference field is formed according to (7).

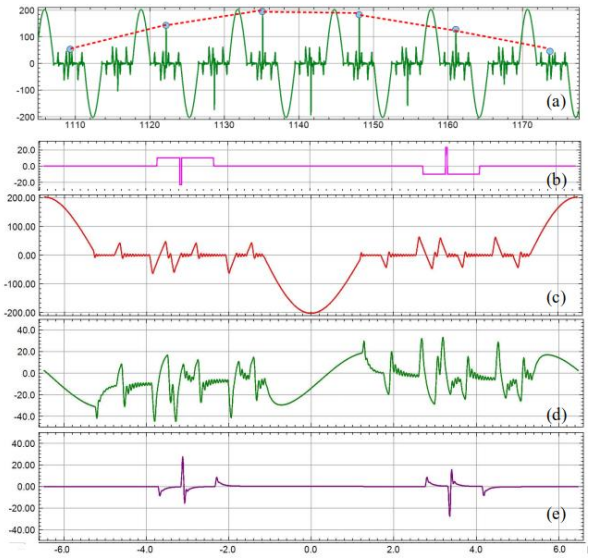

Figure 3. Processes and signals before and after measuring conversion

Figure 3 shows the sequence of signal transformations: (a) – linear superposition at the measuring system input of the reference (b) and main (c) processes, the dotted line shows the modulation of the reference process; at (d) and (e) we can see time-domain forms of the main and reference processes after separation respectively.

Figure 4 explains the calculation according to (9) for the frequency response of the measuring conversion. There are spectra for both known reference process at the input (a) and for the signal obtained at the output of the measuring transformations (b). The graph (c) in the spectral form shows the shape of measuring system frequency response (only the amplitude part of spectrum is shown).

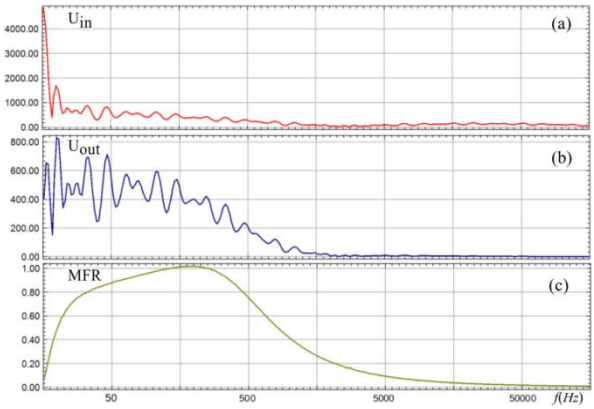

Figure 4 . Calculation of the frequency domain response of the measurement conversion

Figure 5 shows in time-domain the result of the correction performed according to (9)–(10) for all significant harmonics of the spectrum. In the figure: (a) is the input process, (b) is the output signal after the measurement conversion immediately, (c) is the result of the correction.

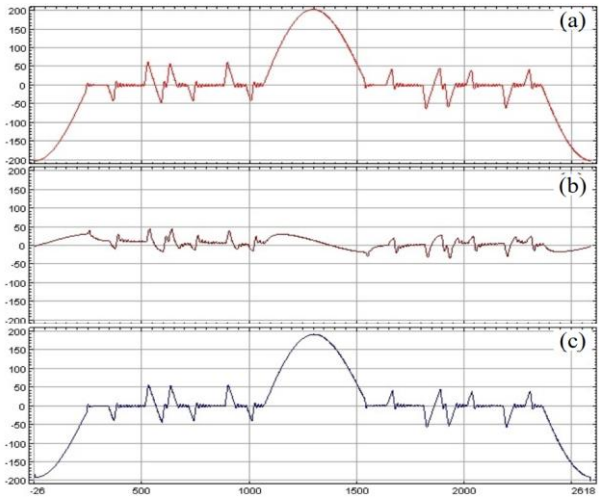

Figure 5. The result of the correction, obtaining the original time domain shape of main process

Figure 6 shows the results of adaptive correction method and algorithm. There are three groups of graphs related to the start, to the survey and the end of the same flight. The upper graphs are the inphase components of the secondary field at 20 harmonics from 77 Hz to 10 kHz (at high altitude must be zero). Under them there are the quadrature components (also zero at high altitude). Next there are 14 channels of *dB*/*dt* for the big pulse in figure 5 in time domain. The lowest graphs show the flight altitude above the ground. We can see that the values of the secondary field both in time an frequency domain at high altitude equal zero, and due to use of the adaptive correction after six hours flight the phase of the measured signal remain the same.

CONCLUSIONS

We have presented the results of development and implementation of the adaptive correction method and algorithm. We have shown functioning stability of AEM system EQUATOR provided by suggested approach. In our opinion, the versatility of the approach and the simplicity of technical implementation make it possible to apply the proposed method and algorithm in many well known AEM systems.

REFERENCES

Hamming, R., 2013. Digital filters. Dover Publications.

Legault, J.M., 2015. Airborne electromagnetic systems – state of the art and future directions. CSEG recorder 40 (6): 38-49.

Macnae, J., 2016. Quantitative estimation of intrinsic induced polarization and superparamagnetic parameters from airborne electromagnetic data. Geophysics 81 (6): E433-E446.

Wu, X., Xue, G., He, Y., and J. Xue, 2019. Removal of the multi-source noise in airborne electromagnetic data based on deep learning. Geophysics 85(6): 1-72.

Moilanen, J., Karshakov, E., and A. Volkovitsky, 2013. Time-domain helicopter EM System "Equator": resolution, sensitivity, universality. 13th SAGA biennial and 6thInternational AEM conference AEM-2013, Mpumalanga, South Africa, Expanded Abstracts: 1-4.

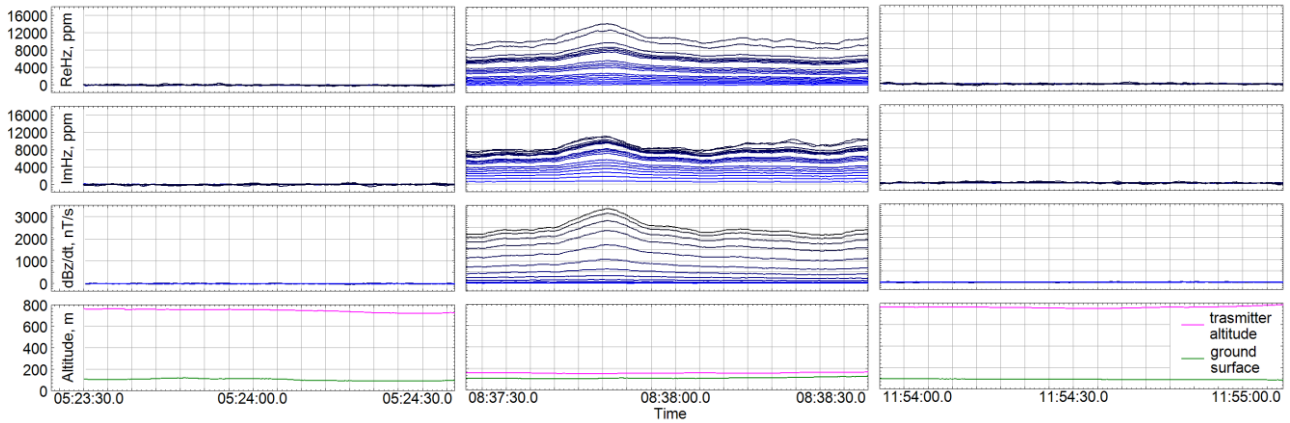

Figure 6. Effectiveness of applying adaptive correction, long-time stability